Table of contents Appendix Figures and Tables

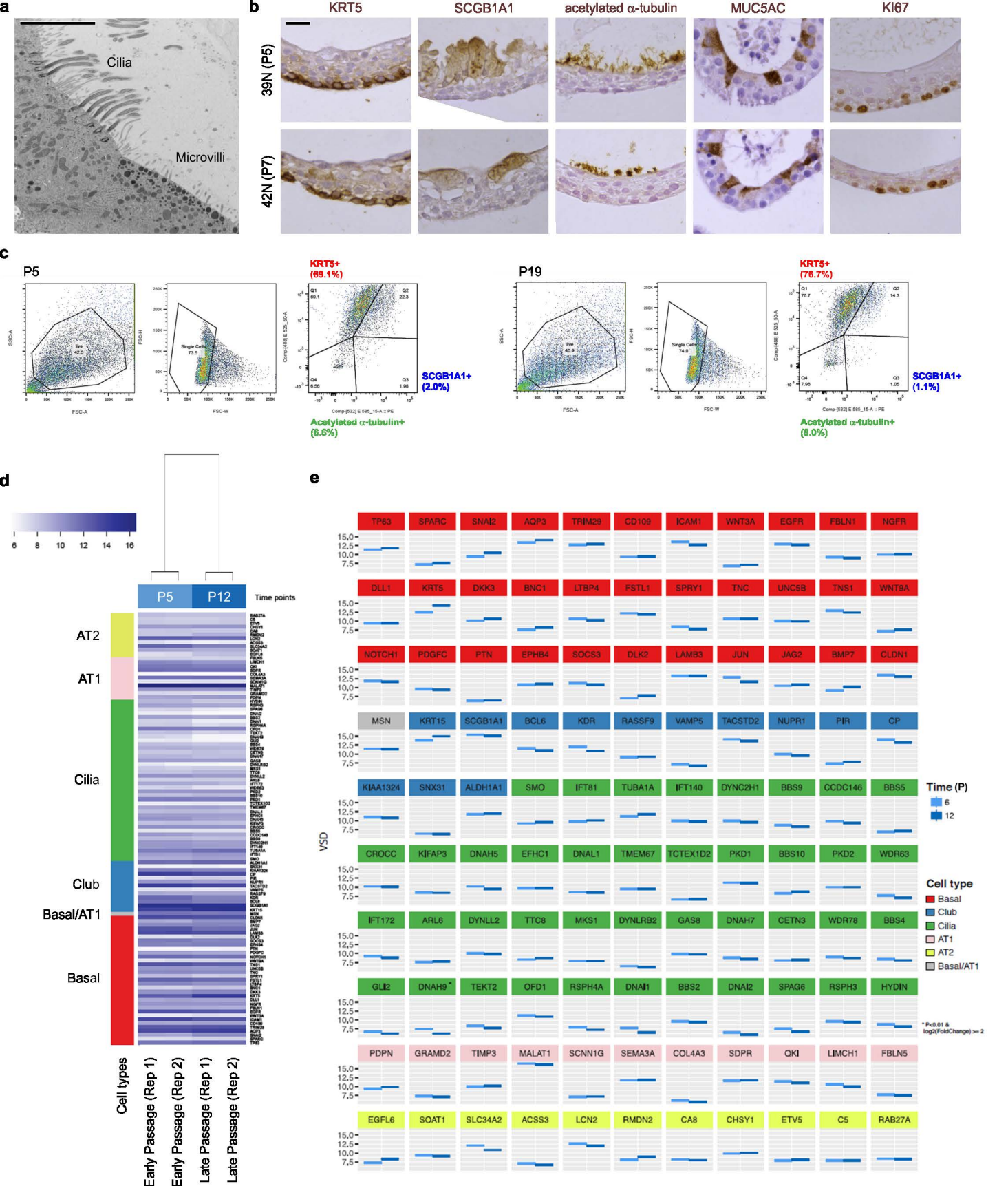
a
Cilia
Microvilli
b
KRT5
SCGB1A1
acetylated α-tubulin
MUC5AC
KI67
39N (P5)
42N (P7)
c
P5
KRT5+ (69.1%)
SCGB1A1+ (2.0%)
Acetylated α-tubulin+ (6.6%)
P19
KRT5+ (76.7%)
SCGB1A1+ (1.1%)
Acetylated α-tubulin+ (8.0%)
d
P5
P12
Time points
AT2
AT1
Cilia
Club
Basal/AT1
Basal
Cell types
Early Passage (Rep 1)
Early Passage (Rep 2)
Late Passage (Rep 1)
Late Passage (Rep 2)
e
VSD
TP63 SPARC SNAI2 AQP3 TRIM29 CD109 ICAM1 WNT3A EGFR FBLN1 NGFR
DLL1 KRT5 DKK3 BNC1 LTBP4 FSTL1 SPRY1 TNC UNC5B TNS1 WNT9A
NOTCH1 PDGFC PTN EPHB4 SOCS3 DLK2 LAMB3 JUN JAG2 BMP7 CLDN1
MSN KRT15 SCGB1A1 BCL6 KDR RASSF9 VAMP5 TACSTD2 NUPR1 PIR CP
KIAA1324 SNX31 ALDH1A1 SMO IFT81 TUBA1A IFT140 DYNC2H1 BBS9 CCDC146 BBS5
CROCC KIFAP3 DNAH5 EFHC1 DNAL1 TMEM67 TCTEX1D2 PKD1 BBS10 PKD2 WDR63
IFT172 ARL6 DYNLL2 TTC8 MKS1 DYNLRB2 GAS8 DNAH7 CETN3 WDR78 BBS4
GLI2 DNAH9* TEKT2 OFD1 RSPH4A DNAI1 BBS2 DNAI2 SPAG6 RSPH3 HYDIN
PDPN GRAMD2 TIMP3 MALAT1 SCNN1G SEMA3A COL4A3 SDPR QKI LIMCH1 FBLN5
EGFL6 SOAT1 SLC34A2 ACSS3 LCN2 RMDN2 CA8 CHSY1 ETV5 C5 RAB27A
Time (P)
6
12
Cell type
Basal
Club
Cilia
AT1
AT2
Basal/AT1
* P<0.01 & log2(FoldChange) >= 2

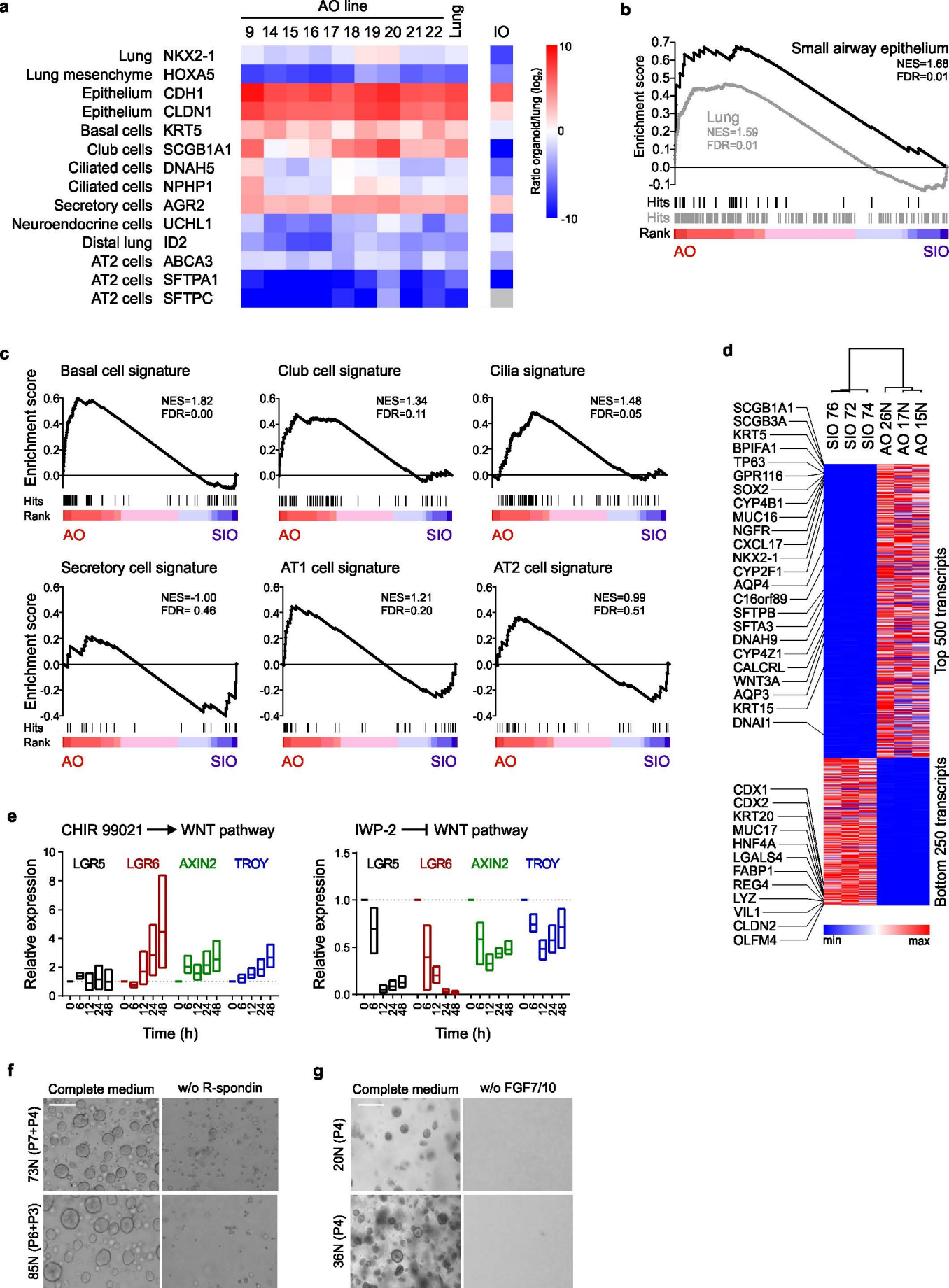
a
AO line
9 14 15 16 17 18 19 20 21 22
Lung
IO
Lung NKX2-1
Lung mesenchyme HOXA5
Epithelium CDH1
Epithelium CLDN1
Basal cells KRT5
Club cells SCGB1A1
Ciliated cells DNAH5
Ciliated cells NPHP1
Secretory cells AGR2
Neuroendocrine cells UCHL1
Distal lung ID2
AT2 cells ABCA3
AT2 cells SFTPA1
AT2 cells SFTPC
Ratio organoid/lung (log2)
10
0
-10
b
Small airway epithelium
NES=1.68
FDR=0.01
Lung
NES=1.59
FDR=0.01
Enrichment score
Hits
Rank
AO
SIO
c
Basal cell signature
NES=1.82
FDR=0.00
Club cell signature
NES=1.34
FDR=0.11
Cilia signature
NES=1.48
FDR=0.05
Secretory cell signature
NES=-1.00
FDR= 0.46
AT1 cell signature
NES=1.21
FDR=0.20
AT2 cell signature
NES=0.99
FDR=0.51
d
SIO 76
SIO 72
SIO 74
AO 26N
AO 17N
AO 15N
SCGB1A1
SCGB3A
KRT5
BPIFA1
TP63
GPR116
SOX2
CYP4B1
MUC16
NGFR
CXCL17
NKX2-1
CYP2F1
AQP4
C16orf89
SFTPB
SFTA3
DNAH9
CYP4Z1
CALCRL
WNT3A
AQP3
KRT15
DNAI1
CDX1
CDX2
KRT20
MUC17
HNF4A
LGALS4
FABP1
REG4
LYZ
VIL1
CLDN2
OLFM4
Top 500 transcripts
Bottom 250 transcripts
min
max
e
CHIR 99021 → WNT pathway
IWP-2 ⊣ WNT pathway
LGR5
LGR6
AXIN2
TROY
Relative expression
Time (h)
f
Complete medium
w/o R-spondin
73N (P7+P4)
85N (P6+P3)
g
Complete medium
w/o FGF7/10
20N (P4)
36N (P4)

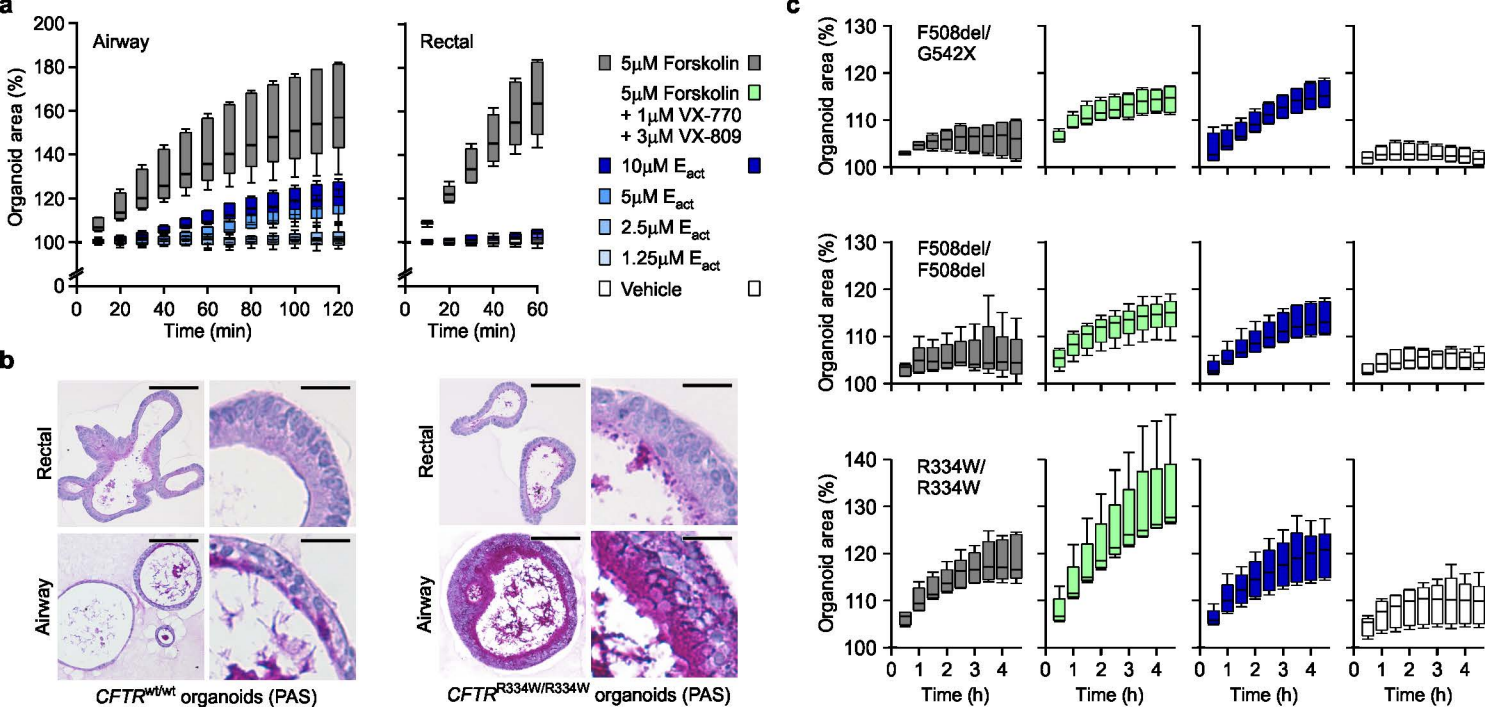
a
Airway
Rectal
Organoid area (%)
Time (min)
5μM Forskolin
5μM Forskolin + 1μM VX-770 + 3μM VX-809
10μM Eact
5μM Eact
2.5μM Eact
1.25μM Eact
Vehicle
b
Rectal
Airway
CFTRwt/wt organoids (PAS)
CFTRR334W/R334W organoids (PAS)
c
F508del/ G542X
F508del/ F508del
R334W/ R334W
Organoid area (%)
Time (h)

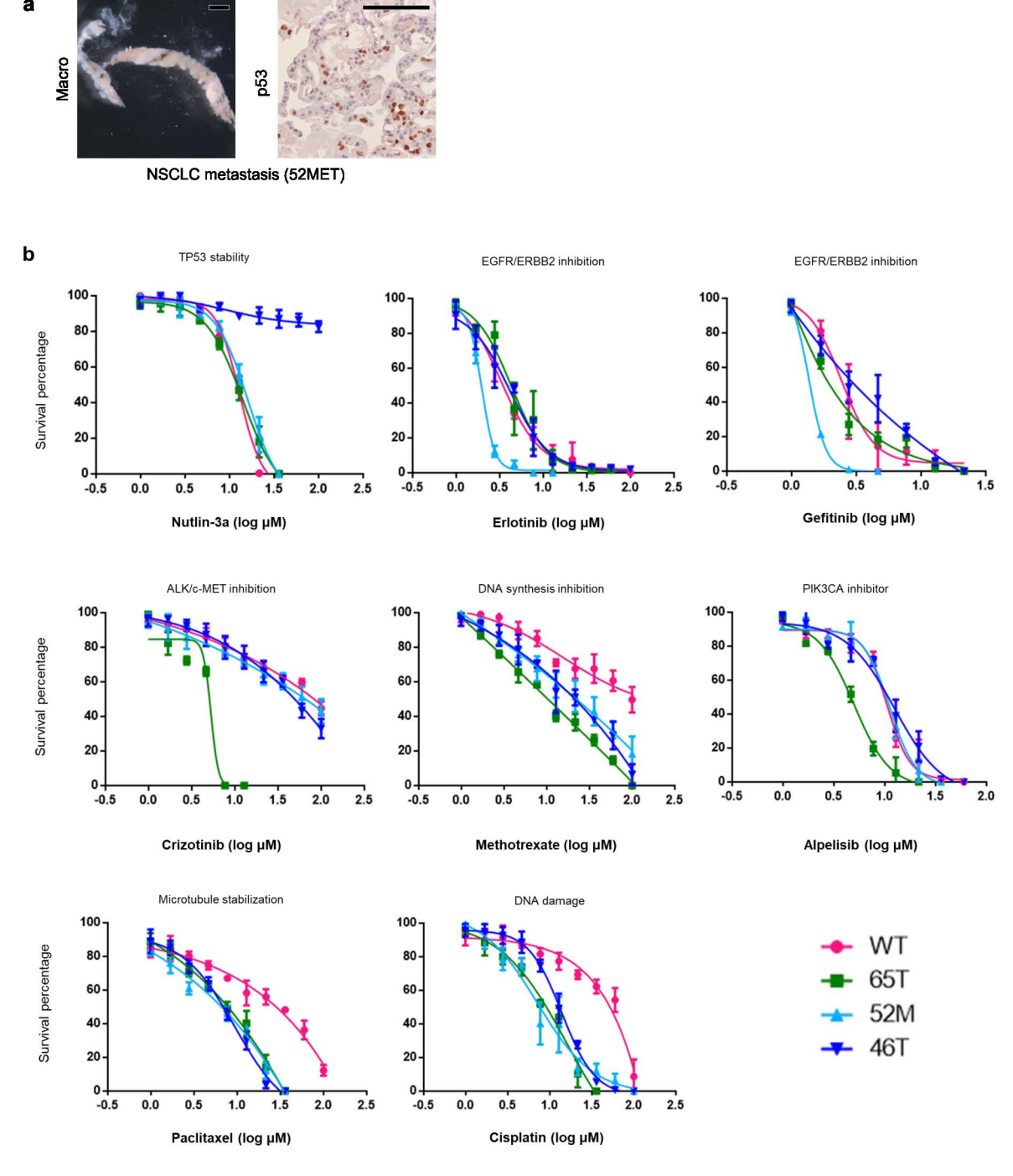
a
Macro
p53
NSCLC metastasis (52MET)
b
TP53 stability
EGFR/ERBB2 inhibition
EGFR/ERBB2 inhibition
Survival percentage
Nutlin-3a (log μM)
Erlotinib (log μM)
Gefitinib (log μM)
ALK/c-MET inhibition
DNA synthesis inhibition
PIK3CA inhibitor
Crizotinib (log μM)
Methotrexate (log μM)
Alpelisib (log μM)
Microtubule stabilization
DNA damage
Paclitaxel (log μM)
Cisplatin (log μM)
WT
65T
52M
46T

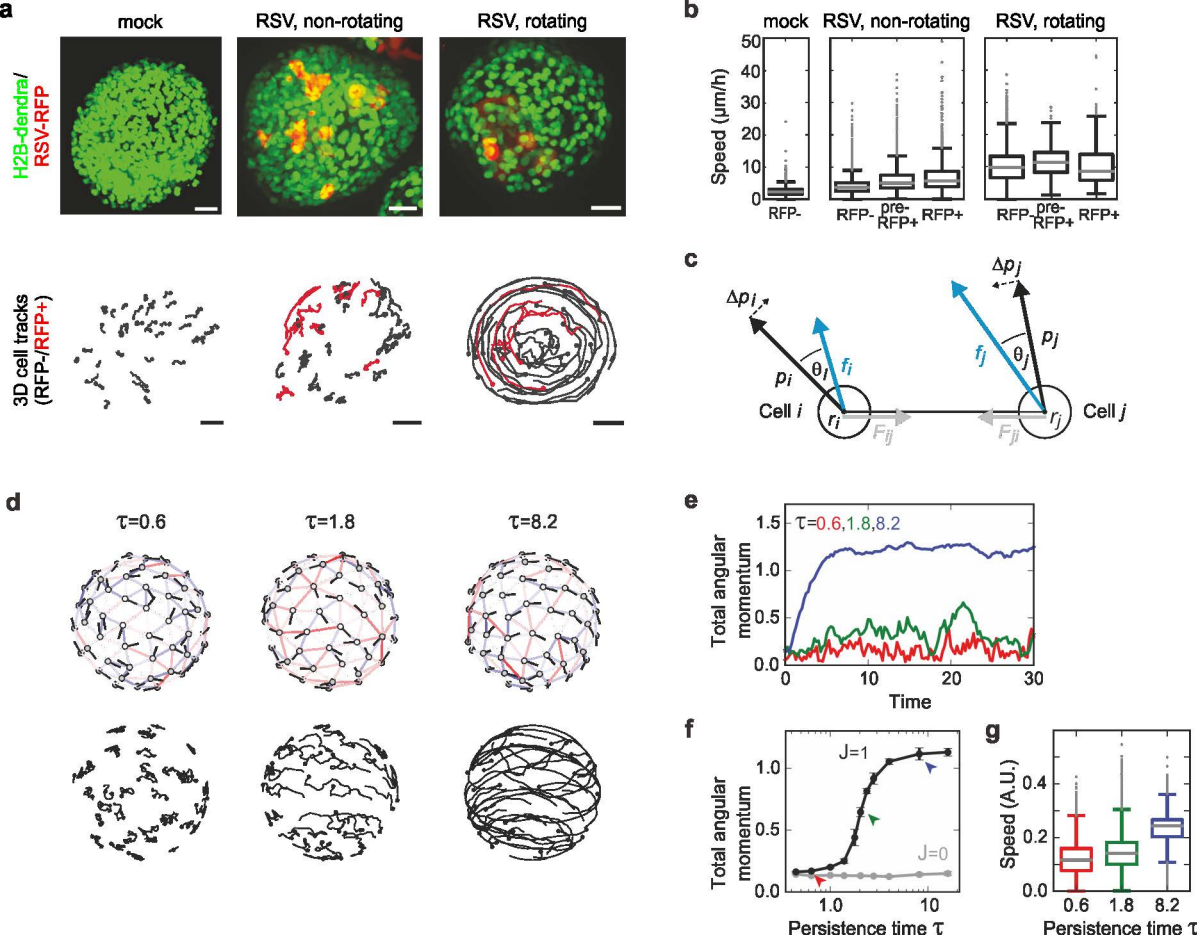
a
mock
RSV, non-rotating
RSV, rotating
H2B-dendra/
RSV-RFP
3D cell tracks
(RFP-/RFP+)
b
mock
RSV, non-rotating
RSV, rotating
Speed (μm/h)
50
40
30
20
10
0
RFP-
RFP-
pre-
RFP+
RFP+
RFP-
pre-
RFP+
RFP+
c
Δp_i
Δp_j
p_i
f_i
θ_i
Cell i
r_i
F_ij
f_j
p_j
θ_j
F_ji
r_j
Cell j
d
τ=0.6
τ=1.8
τ=8.2
e
τ=0.6,1.8,8.2
Total angular
momentum
1.5
1.0
0.5
0.0
0
10
20
30
Time
f
J=1
J=0
Total angular
momentum
1.0
0.5
0.0
1.0
10
Persistence time τ
g
Speed (A.U.)
0.4
0.2
0.0
0.6
1.8
8.2
Persistence time τ

a

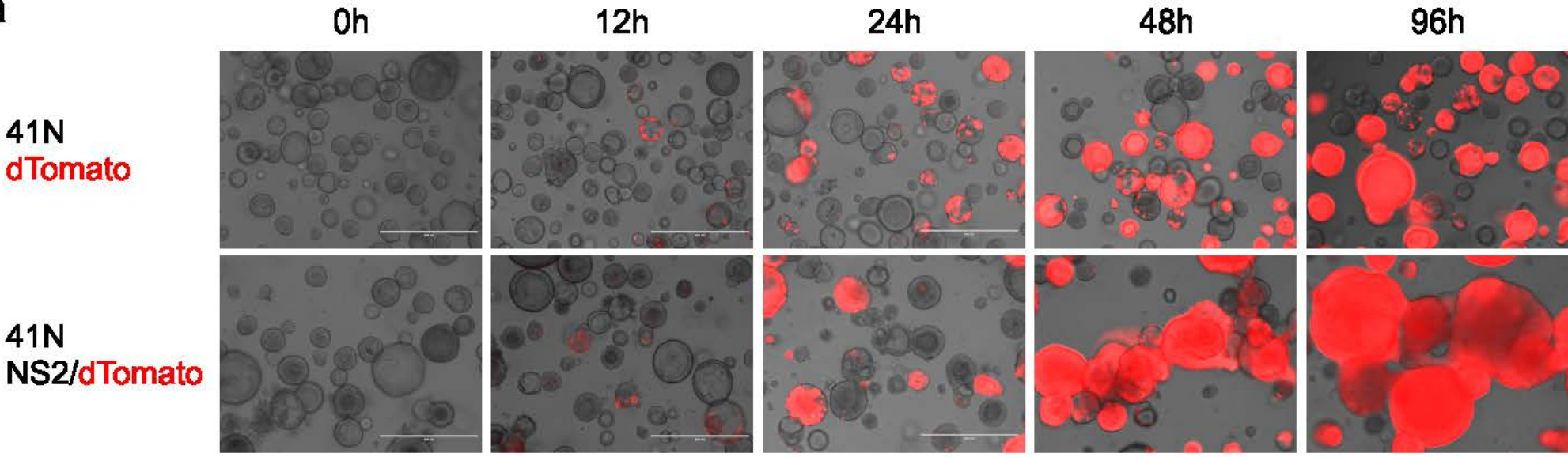
0h
12h
24h
48h
96h
41N
dTomato
41N
NS2/dTomato

b

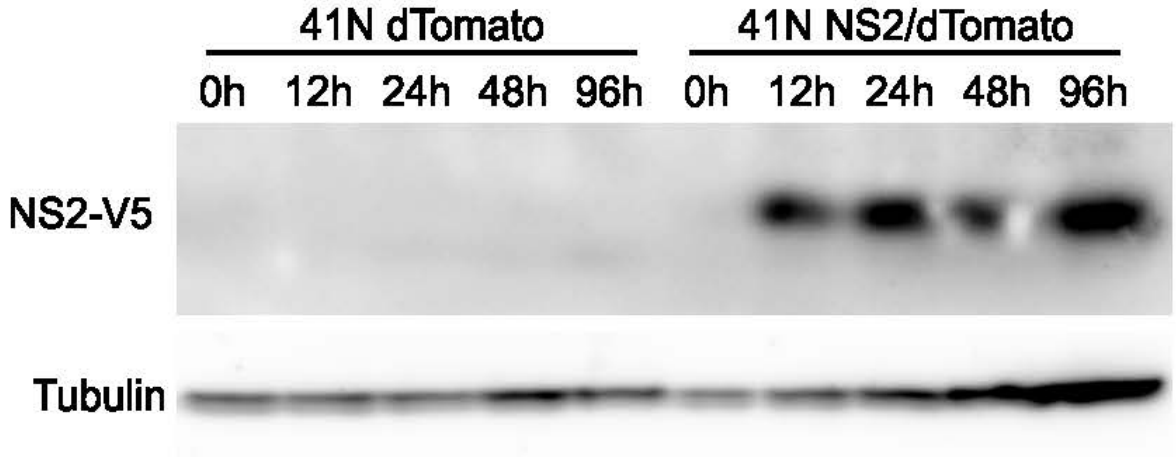
41N dTomato
41N NS2/dTomato
0h 12h 24h 48h 96h 0h 12h 24h 48h 96h
NS2-V5
Tubulin

Appendix Table S1: Cancer gene mutations as identified by WGS

SAMPLE_correc	CHROM	LOCATION	COSMIC_ID	REF	ALT	FILTER	VARIANT_TYPE	SNPEFF_ANN_	GENE	TRANSCRIPT	PROTEIN_CODING
57T-organoid	7	81689805	COSM1199352	C	T	PASS	missense_variant	MODERATE	CACNA2D1	ENSG00000153956	ENST00000356253
57T-tumor	7	81689805	COSM1199352	C	T	PASS	missense_variant	MODERATE	CACNA2D1	ENSG00000153956	ENST00000356253
57T-organoid	7	97860573	COSM3394967	C	T	PASS	missense_variant	MODERATE	TECPR1	ENSG00000205356	ENST00000379795
57T-tumor	7	97860573	COSM3394967	C	T	PASS	missense_variant	MODERATE	TECPR1	ENSG00000205356	ENST00000379795
57T-organoid	19	6904145	COSM3541132	C	T	PASS	missense_variant	MODERATE	EMR1	ENSG00000174837	ENST00000312053
57T-tumor	19	6904145	COSM3541132	C	T	PASS	missense_variant	MODERATE	EMR1	ENSG00000174837	ENST00000312053
65T-organoid	14	75373806	COSM3690200	G	A	PASS	missense_variant	MODERATE	RPS6KL1	ENSG00000198208	ENST00000358328
57T-tumor	14	75373806	COSM3690200	G	A	PASS	missense_variant	MODERATE	RPS6KL1	ENSG00000198208	ENST00000358328
57T-organoid	6	90428228	COSM3876101	C	T	PASS	stop_gained	HIGH	MDN1	ENSG00000112159	ENST00000369393
57T-tumor	6	90428228	COSM3876101	C	T	PASS	stop_gained	HIGH	MDN1	ENSG00000112159	ENST00000369393
65T-organoid	10	46121887	COSM4014278	G	A	PASS	missense_variant	MODERATE	ZFAND4	ENSG00000172671	ENST00000344646
65T-tumor	10	46121887	COSM4014278	G	A	PASS	missense_variant	MODERATE	ZFAND4	ENSG00000172671	ENST00000344646
65T-organoid	2	29940449	COSM4312739	C	T	PASS	missense_variant	MODERATE	ALK	ENSG00000171094	ENST00000389048
65T-tumor	2	29940449	COSM4312739	C	T	PASS	missense_variant	MODERATE	ALK	ENSG00000171094	ENST00000389048
65T-organoid	17	2995561	COSM4506832	G	A	PASS	missense_variant	MODERATE	OR1D2	ENSG00000184166	ENST00000331459
65T-tumor	17	2995561	COSM4506832	G	A	PASS	missense_variant	MODERATE	OR1D2	ENSG00000184166	ENST00000331459
57T-organoid	9	74309501	COSM4588918	T	C	PASS	missense_variant	MODERATE	TMEM2	ENSG00000135048	ENST00000377044
57T-tumor	9	74309501	COSM4588918	T	C	PASS	missense_variant	MODERATE	TMEM2	ENSG00000135048	ENST00000377044
57T-organoid	20	10036179	COSM4661930	G	T	PASS	missense_variant	MODERATE	ANKEF1	ENSG00000132623	ENST00000378380
65T-organoid	9	133942352	COSM4697377	C	T	PASS	missense_variant	MODERATE	LAMC3	ENSG00000050555	ENST00000361069
65T-tumor	9	133942352	COSM4697377	C	T	PASS	missense_variant	MODERATE	LAMC3	ENSG00000050555	ENST00000361069
65T-tumor	19	15794307	COSM4988566	C	T	PASS	missense_variant	MODERATE	CYP4F12	ENSG00000186204	ENST00000324632
57T-organoid	3	49699942	COSM5087506	G	A	PASS	missense_variant	MODERATE	BSN	ENSG00000164061	ENST00000296452
57T-tumor	3	49699942	COSM5087506	G	A	PASS	missense_variant	MODERATE	BSN	ENSG00000164061	ENST00000296452
65T-organoid	6	49808659	COSM5173147	C	T	PASS	missense_variant	MODERATE	CRISP1	ENSG00000124812	ENST00000335847
65T-tumor	6	49808659	COSM5173147	C	T	PASS	missense_variant	MODERATE	CRISP1	ENSG00000124812	ENST00000335847
65T-organoid	16	15141904	COSM5213311	C	T	PASS	missense_variant	MODERATE	NTAN1	ENSG00000157045	ENST00000287706
65T-tumor	16	15141904	COSM5213311	C	T	PASS	missense_variant	MODERATE	NTAN1	ENSG00000157045	ENST00000287706
57T-organoid	17	10225010	COSM5385616	C	T	PASS	missense_variant	MODERATE	MYH13	ENSG00000006788	ENST00000252172
57T-tumor	17	10225010	COSM5385616	C	T	PASS	missense_variant	MODERATE	MYH13	ENSG00000006788	ENST00000252172
57T-organoid	10	94836819	COSM921543	C	T	PASS	stop_gained	HIGH	CYP26A1	ENSG00000095596	ENST00000224356
57T-organoid	17	15531954	COSM975785	G	A	PASS	missense_variant	MODERATE	TRIM16	ENSG00000221926	ENST00000336708
57T-tumor	17	15531954	COSM975785	G	A	PASS	missense_variant	MODERATE	TRIM16	ENSG00000221926	ENST00000336708

Appendix Table S2: Hotspot cancer gene sequencing results

	46T	47T	51T	52MET	52METII	53MET	60MET
ABL1							
AKT1							
ALK							
APC							
ATM							
BRAF							
BRCA1							
BRCA2							
CDH1							
CDKN2A							
CSF1R							
CTNNB1							
EGFR			p.(Leu858Arg) 81.87%				
ERBB2				p.(Gly776Ser) 66.77%	p.(Gly776Ser) 70.41%		
ERBB2				p.(Gly778_Ser779 insSer) 66.67%	p.(Gly778_Ser779 insSer) 68.78%		
ERBB4							
EZH2							
FBXW7							
FGFR1							
FGFR2							
FGFR3							
FLT3							
GNA11							
GNAQ							
GNAS							
HNF1A							
HRAS							
IDH1							
IDH2							
JAK2							
JAK3							
KDR							
KIT							
KRAS		p.(Gly12Val) 49.96%					
MET							
MLH1							
MPL							
NOTCH1							
NPM1							
NRAS							
PDGFRA							
PIK3CA							
PTEN							
PTPN11							
RB1							
RET							
SMAD4							
SMARCB1							
SMO							
SRC							
STK11	p.(Glu165X) 100%	p.(Glu165X) 100%					
TP53	p.(Arg248Trp) 100%	p.(Asp281Glu) 100%				p.(Phe212SerfsTer3) 51.07%	p.(Arg273His) 7.91%
TP53							p.(Tyr220Cys) 15.77%
VHL							

Appendix Table S3: Sequence of used qPCR primers.

q-PCR primers	FW	REV
HRPT	5’-AAGAGCTATTGTAATGACCAGT-3’	5’-CAAAGTCTGCATTGTTTTGC-3’
NKX2-1	5’-ACCAAGCGCATCCAATCTCA-3’	5’-CAGAGCCATGTCAGCACAGA-3’
HOXA5	5’-CGAGCCACAAATCAAGCACA-3’	5’-GAATTGCTCGCTCACGGAAC-3’
CDH1	5’-TTACTGCCCCCAGAGGATGA-3’	5’-TGCAACGTCGTTACGAGTCA-3’
CLDN1	5’-CTGTCATTGGGGGTGCGATA-3’	5’-CTGGCATTGACTGGGGTCAT-3’
KRT5	5’-GCATCACCGTTCCTGGGTAA-3’	5’-GACACACTTGACTGGCGAGA-3’
SCGB1A1	5’-TCCTCCACCATGAAACTCGC-3’	5’-AGGAGGGTTTCGATGACACG-3’
DNAH5	5’-AGAGGCCATTCGCAAACGTA-3’	5’-CCCGGAAAATGGGCAAACTG-3’
NPHP1	5’-CAGAGCCACATGGCAACCTA-3’	5’-ACCCAGCCACAGCTTAACTC-3’
AGR2	5’-TCAGAAGCTTGGACCGCATC-3’	5’-AGTGTAGGAGAGGGCCACAA-3’
UCHL1	5’-GACGAATGCCTTTTCCGGTG-3’	5’-AGAAGCGGACTTCTCCTTGC-3’
ID2	5’-GCAGCACGTCATCGACTACA-3’	5’-TTCAGAAGCCTGCAAGGACA-3’
ABCA3	5’-CACCAGGGGCTCTCTAGACT-3’	5’-ACAGCCATCGTCTTGCTGAA-3’
SFTPA1	5’-CAGACGGGACCCCTGTAAAC-3’	5’-CCTGTCATTCCACTGCCCAT-3’
SFTPC	5’-ATGGATGTGGGCAGCAAAGA-3’	5’-CAGCAGGGAATGCCAAATCG-3’
LGR5	5’-CACCGCTCTCAGTCACTGGATAAGC-3’	5’-AAACGCTTATCCAGTGACTGAGAGC-3’
LGR6	5’-CCAAGGACAGTTTCCCAAAA-3’	5’-GACTCCTCATCATCAAGGTGAA-3’
AXIN2	5’-AGCTTACATGAGTAATGGGG-3’	5’-AATTCCATCTACACTGCTGTC-3’
TROY	5’-TGATGAAAGTAGGCAGGGCTGTGT-3’	5’-TCTCCAGCCAGTGTTTGTCCTTGA-3’

Appendix **Figure S 1. Further characterization of airway organoids.**

a, Transmission electron micrograph showing a multi-ciliated cell next to a cell with microvilli and apical vesicles. Scale bar equals 2µm. See also Movie EV 1.

b, Immunohistochemical analysis of AO lines 39 and 42. Shown are markers of basal cells (KRT5), club cells (SCGB1A1), multi-ciliated cells (acetylated α-tubulin), secretory cells (MUC5AC), and proliferation (KI67). Scale bar equals 5µm. Micrographs have been rotated and cropped to align epithelia resulting in the cropped edge of 39N SCGB1QA1.

c, Quantification of cell types in AO lines at early and late passage (P5 vs P19) as determined by flow cytometry using the indicated markers. The number of basal cells, club cells, ciliated cells, and secretory cells does not differ significantly between early and late passage AOs.

d, **e**, RNA sequencing of early (5) vs late (12) AOs indicates similar expression of cell type specific marker genes. Shown is a heat map comparing the expression levels of lineage markers (**d**) as well as detailed expression levels of selected markers (**e**). Variance Stabilizing Transformed (VSD) values are plotted to facilitate comparison across different markers. See Table 2.

Appendix **Figure S 2. Further characterization of airway organoids.**

a, Heat map showing qPCR results of marker gene expression in ten individual AO lines compared to whole lung and one intestinal organoid line. Data are shown as $\log_2$-transformed ratio of sample over whole lung. AOs express lung cell marker *NKX2-1* at comparable levels to whole lung (pale blue to pale red), while being negative for lung mesenchymal marker gene *HOXA5* (dark blue) and strongly positive for general epithelial markers *CDH1* and *CLDN1* (dark red). AOs furthermore express relatively more *KRT5* (basal cell marker), *SCGB1A1* (club cell marker), and *AGR2* (secretory cell marker). Ciliated cell markers *DNAH5* and *NPHP1* are expressed at similar levels in AOs and whole lung (pale blue to pale red). AOs express less of neuroendocrine marker UCHL1, distal lung marker ID2, and AT2 markers *ABCA3*, *SFTPA1*, and *SFTPC* (white to dark blue). The intestinal organoid line is positive for

epithelial, basal, and secretory cell markers (pale red to red), and negative for general lung, lung mesenchyme, club cell, ciliated cell, neuroendocrine cell, distal lung, and AT2 cell markers (pale blue to dark blue).

b, GSEA plots showing strong enrichment of small airway epithelium and lung gene signatures in transcriptomes of three AO lines compared to three small intestinal organoid (SIO) lines. NES = normalized enrichment score, FDR = false discovery rate. See Table 3.

c, Top row: GSEA plots showing enrichment of gene signatures of basal cells, cilia, and club cells in transcriptomes of three AO lines compared to three small intestinal organoid (SIO) lines. Bottom row: GSEA plots showing no enrichment of gene signatures of secretory cells, AT1 cells, and AT2 cells in the same data set. NES = normalized enrichment score, FDR = false discovery rate. See Table 3 for signatures and leading-edge genes.

d, Hierarchical clustering of the indicated AO and SIO lines. Analysis is based on the top 500 and bottom 250 expressed genes in averaged AO vs SIO transcripts (full list in Table 3). Gradients depict the relative maximum and minimum values per transcript. Names and ranks of signature lung and intestinal genes are indicated.

e, Box and Whiskers plots showing changes in the expression of WNT target genes over time following manipulation of the WNT pathway. Upon strong activation of the WNT pathway using GSK-3 inhibitor CHIR 99021, *LGR5* expression remains unaltered, while expression of *AXIN2* and *TROY* is moderately and expression of *LGR6* is strongly increased. Upon blocking the WNT pathway with porcupine inhibitor IWP-2, *LGR5* and *LGR6* expression drops sharply, while *AXIN2* and *TROY* expression is decreased moderately. Analysis is based on three independent experiments using AO lines 15, 17, and 26. Whiskers indicate smallest and largest values, boxes indicate 25^{th} to 75^{th} percentile, horizontal solid line indicates median.

f, Phase contrast images of two independent AO lines grown in the presence and absence of R-spondin. After 3-4 passages without R-spondin, AOs cannot be expanded further (right column). Scale bar equals 100 μm.

g, Phase contrast images of two independent AO lines grown in the presence and absence of FGF-7 and FGF-10. After 4 passages without FGFs, no AOs remain in culture (right column). Scale bars equals 100µm.

Appendix Figure S 3. Additional data of airway organoids to study cystic fibrosis.

a, Box-and-Whisker plots showing organoid swelling over time following stimulation with forskolin or E_{act}. While forskolin causes swelling in both organoid types (grey boxes), E_{act} causes concentration-dependent swelling only of AOs (blue hued boxes). Shown are pooled data from three different AO and two different rectal organoid lines used in three to four independent experiments. See Figure 2a, b for the respective AUC plots. Whiskers indicate smallest and largest values, boxes indicate 25th to 75th percentile, horizontal solid line indicates median.

b, Representative histological sections of PAS-stained wild-type organoids (unmatched, left panel) and organoids from a CF patient with *CFTR*$^{R334W/R334W}$ mutation (right panel). PAS-positive mucus is occasionally present within wild-type AOs but not rectal wild-type organoids, while the CF patient AOs regularly show thick layers of PAS-positive mucus. Rectal organoids from the same CF patient display only occasional regions with PAS-positive mucus. Rectal organoids were generated from rectal biopsies, AOs were generated from lung resection (wild-type) or BAL-fluid (CF patient). Scale bars equal 50 µm (overviews) and 10 µm (details). See Figure 2c for PAS-stained *CFTR*$^{F508del/F508del}$ organoid sections.

c, Box-and-Whisker plots showing CF patient AO swelling over time following addition of the indicated stimuli. The respective CFTR mutations are given atop every row of plots. Forskolin-induced swelling (grey boxes) does not exceed vehicle controls in AOs with *CFTR*$^{F508del/G542X}$ and *CFTR*$^{F508del/F508del}$ genotypes, but increases in the presence of VX-770 and VX-809 (green boxes). In the same organoids, E_{act}-induced swelling (blue boxes) exceeds forskolin-induced swelling to a similar extend. AOs with the milder *CFTR*$^{R334W/R334W}$ genotype (bottom row) show moderate forskolin-induced swelling that is increased in the presence of VX-770 and VX-809 and paralleled by E_{act}-induced swelling. Shown are pooled data of four to five independent experiments. See Figure 2d for the corresponding AUC-plots. Whiskers

indicate smallest and largest values, boxes indicate 25th to 75th percentile, horizontal solid line indicates median.

Appendix **Figure S 4. Additional data of tumor airway organoids.**

a, Macroscopic photograph of a NSCLC metastasis biopsy and p53 immunohistochemistry of the derived tumor AO line 52MET. Scale bars equal 2 mm and 200 μm.

b, Shown are dose response curves of several AO lines treated with erlotinib, gefitinib (both targeting EGFR/ERBB2 mutations), crizotinib (targeting ALK mutations), methotrexate (targeting DNA synthesis), paclitaxel (targeting microtubule disassembly), Nutlin-3a (stabilizing p53), alpelisib (targeting PIK3CA mutations), and cisplatin (inducing DNA damage). See Figure 3d for a summarizing heat map of the corresponding logIC_{50} values. Data shown are representatives of at least 3 independent experiments. Error bars indicate s.e.m.

Appendix Figure S 5. Single cell velocities of RSV-infected AOs and mathematical modelling of organoid rotation.

a, Examples of non-infected (left), RSV-infected and non-rotating (middle), and RSV-infected and rotating (right) organoids with the corresponding tracks of randomly selected nuclei (n=41, 33, 35 respectively). Track durations are 14 h. Circles indicate the starting position of each track, and line color stands for either RPF- (black) or RFP+ (red) cells. Scale bars represent 25μm.

b, Tukey Box plots of the speed distribution of every tracked nucleus at each time point for non-infected (n=3), infected but non-rotating (n=6) and infected and rotating (n=3) organoids, where 15-45 individual nuclei were tracked per organoid. For the infected organoids, nuclei were classified as RFP- when they showed no RFP signal for the duration of the track, pre-RFP+ when the nuclei showed no RFP signal yet but became RFP+ later, and RFP+ for nuclei that showed RFP signal. Horizontal solid line indicate median box, box indicates 25th to 75th percentile, whiskres indicate 25th percentile minus 1.5 times inter-quartile distance (IQR) or 75th percentile plus 1.5 times IQR, circles indicate individual values greater than 1.5 times IQR.

c, Vector schematic depicting the modelled relation between cells migrating within the constraints of an organoid sphere. See Methods and Protocols for details.

d, Snapshots of the cell configuration (left) and cell tracks (right) for simulations with n=100 cells and increasing persistence time τ=0.6, 1.8 and 8.2. The persistence time indicates the mean time over which the cell maintains its direction of polarization, in the absence of cell-cell interactions. White markers represent cell centres, with black lines showing the direction of the polarization vector. Adjacent cells are connected by springs, which are shown as coloured lines. Springs are red when stretched and blue when compressed. Cell tracks are shown for the same time period for all three simulations, with black circles indicating the starting position of each track. See also **Movie EV** 7.

e, Total angular momentum of the cell configuration as a function of time for simulations starting with random initial distribution of polarity vectors. For sufficiently high persistence time ($\boldsymbol{\tau}$=8.2, blue line), the cells rapidly establish rotational motion.

f, Total steady state angular momentum as function of the persistence time $\boldsymbol{\tau}$, for simulations with cell-cell communication (black, $\boldsymbol{J}$=1) and without (grey, $\boldsymbol{J}$=0). Coloured arrows indicate the persistence times corresponding to the simulations in panel e.

g, Box plots of the distribution of cell speed for the different persistence times in panel (E). The distribution is calculated from n=5 independent simulations. Horizontal solid line indicates median, box indicates 25th to 75th percentile, whiskers indicate 25th percentile minus 1.5 times inter-quartile distance (IQR) or 75th percentile plus 1.5 times IQR, circles indicate individual values greater than 1.5 times IQR.

Appendix Figure S 6. Inducible expression of NS2 in AOs.

a, Brightfield/fluorescent micrographs of AOs inducibly overexpressing dTomato (top) or NS2 and dTomato (bottom) taken at the indicated time points following stimulation with doxycycline. While red signal increases in both lines, organoid fusion exclusively takes place in AOs expressing NS2. See **Movie EV** 11. Scale bars equal 400 μm.

b, Western blots of protein lysates from the indicated AOs taken at the indicated time points following stimulation with doxycycline. NS2 protein is robustly detectable after 12h of stimulation.

Appendix ***Tables***

Appendix **Table S 1** – Cancer gene mutations in tumor tissue-AO pairs as identified by WGS

Appendix **Table S 2** – Hotspot cancer gene sequencing of tumoroids

Appendix **Table S 3** – Sequence of used qPCR primers